

THE GEOMETRIC SUPERSITE OF SALON DE PROVENCE

J-M. Delvit^{a,*}, P. Fave^b, R. Gachet^b

^a CNES, DCT/SI/QI, BPI 811, 18 avenue Edouard Belin, 31401 TOULOUSE CEDEX 4, FRANCE –
jean-marc.delvit@cnes.fr

^b IGN Espace, 6 avenue de l'Europe, 31520 RAMONVILLE-SAINT-AGNE, FRANCE –
(pascal.fave,roland.gachet)@ign.fr

Commission I, T11

KEY WORDS: earth observation satellites, image quality, geometry, GPS, aerotriangulation, elevation model, calibration

ABSTRACT:

Since early 1999, the CNES has worked on defining and equipping supersites for its needs in image quality assessment. Various criteria guided the definition of this supersite involving the characteristics of high resolution earth observation satellites and the image quality assessment methods. The main goal of this work was to have a high resolution geometric reference in order to calibrate any high resolution spatial sensor.

A very high resolution camera named PELICAN flew near the city of Salon de Provence in the South East of France in September 2004 and March 2005 to produce images with narrow angular field of view. This site suits geometric and radiometric image quality assessment and moreover ensures an acceptable weather and a stable landscape. Two really different seasons were selected in order to take into account the evolution of the landscape and allow us to calibrate unknown sensors anytime.

The accuracy of sensor calibration that can be obtained using image matching technics depends on several parameters. Both planimetric and altimetric accuracy of reference data over the «supersite» are key factors for the quality of the end result. Altimetry is controlled through an elevation model (including superstructures) whereelse planimetry is controlled through particularly accurate aerotriangulation based on fifty one ground control targets painted and measured with high accuracy through a GPS measurement campaign conducted by an IGN expert in 2004.

As a result, the planimetric accuracy of Salon supersite is better than 5cm RMS. An accurate DEM, at one meter ground resolution has also been computed. Altimetric accuracy of the DEM is better than 10cm RMS.

1. CONTEXT

Since early 1999, the CNES has worked on defining and equipping supersites for its needs in image quality assessment [Gachet 1999], [Gachet 2004]. This paper deals with high resolution geometric reference in order to calibrate any high resolution spatial sensor. This geometric reference is produced by a powerful aerotriangulation based on GPS ground control points and thousands of tie points.

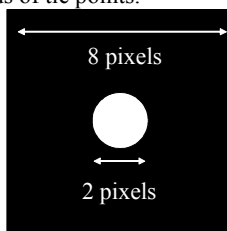


Figure 1 – Target description

radiometric image quality assessment and ensures an acceptable weather. PELICAN is composed of a 4096 by 4196 matrix detector.

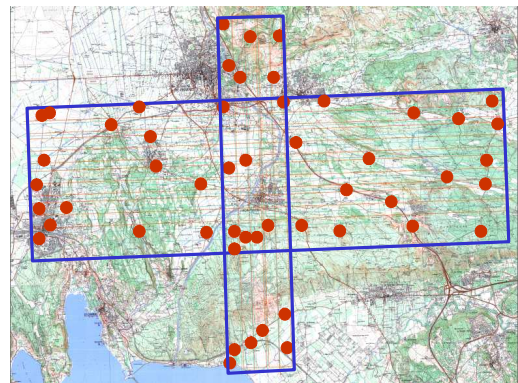


Figure 2 – Target placement through the supersite

2. DATA DESCRIPTION

A very high resolution camera named PELICAN flew near the city of Salon de Provence in the South East of France in September 2004 and March 2005 to produce images with narrow angular field of view. This site suits geometric and

For this study, an East-West band (20km by 6km), composed of 9 bands of 77 aerial images with a longitudinal overlap of 70% and a lateral overlap of 30%, and a North-South band (12km by 3km), composed of 3 bands of 38 images with a longitudinal overlap of 40% and a lateral overlap of 60%, are used. The resolution of used images is about 25cm. The geometry quality

* Corresponding author. Jean-Marc Delvit

of this site can be controlled thanks to 51 ground control targets (Figure 2) which are painted and measured with high accuracy through a GPS measurement campaign. An example of target is described in Figure 1 and one of these targets is shown in situation in Figure 3.



Figure 3 – Example of target within a Pelican image

These ground control points allow us to calibrate the supersite thanks to an aerotriangulation. This aerotriangulation also lies on lots of tie points automatically computed by correlation.

3. AEROTRIANGULATION

3.1 Some definitions

A nadir zone Λ is defined minimizing the distortion effect which covers the swath perpendicularly of the flight direction and 40% of the swath along the flight direction.

A regular grid (Γ) is also defined in this zone. The step of this grid is 40 by 40 pixels, i.e. 40x101 nodes (Figure 4).

Two images have an acceptable covering only if the distance between their two tops of view is less than 1km. The “reference geometry” is the geometry of the reference image and the “secondary geometry” is the geometry of the secondary image. The accurate geometry of the supersite is computed in three steps:

- computing a coarse geometry
- measuring tie points thanks to the coarse geometry
- computing a complete aerotriangulation

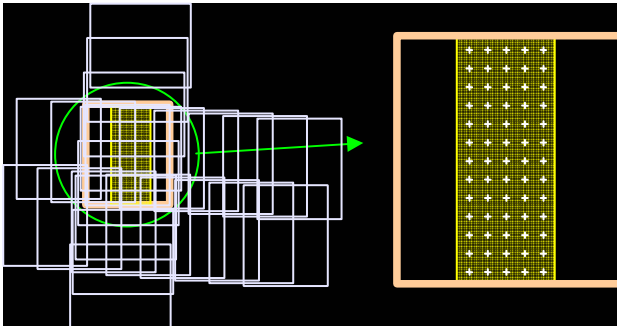


Figure 4 – Description of the covering and Λ

3.2 Coarse geometry calculation

For each “secondary” image which covering is acceptable for the “reference” image the algorithm below is applied:

1. The secondary image is projected in the geometry of the reference image using the native geometric model (trajectory; viewing directions, distortion, ...) with the initial DEM (Figure 13). The sampling grid Γ_s used is phased with the regular grid Γ already defined.
2. An assessment of the roll (R), pitch (P), yaw (Y) and magnification factor (M) is computed from the difference reference/secondary. The covering zone of the two images (Λ for the reference) is divided in two equal parts. For each part (2 couples) measures of translations in the two directions are computed by a linear phase filtering (ΔX_1 , ΔX_2 , ΔY_1 , ΔY_2) as shown in Figure 5. If d is the distance between the centre of each part, and f the focal length, the value of ΔR , ΔP , ΔY , ΔM are updated to:
$$\Delta R = \Delta R + (\Delta Y_1 - \Delta Y_2) / d$$

$$\Delta P = \Delta P + (\Delta X_2 - \Delta X_1) / d$$

$$\Delta Y = \Delta Y + (\Delta X_2 + \Delta X_1) / f$$

$$\Delta M = \Delta M + (\Delta Y_2 + \Delta Y_1) / f$$
3. The geometric model of the reference image is modified according to the new values of ΔR , ΔP , ΔY , ΔM and the algorithm iterates (point 1) until ΔR , ΔP , ΔY , ΔM become stable.

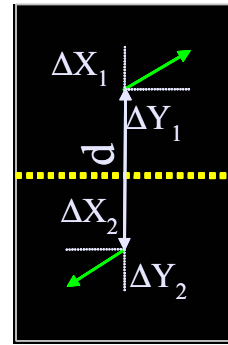


Figure 5 – Translation measurements in the two equal parts of the covering zone

The figures 6 to 10 show an example describing the entire process of the algorithm iteration by iteration.



Figure 6 – Recovering zone: Iteration 1



Figure 7 – Recovering zone: Iteration 2



Figure 8 – Recovering zone: Iteration 3

3.3 Looking for tie points

All the geometric models for all the images in the aerotriangulation block are now better than the original model. Figure 10 shows an example of a useful zone to look for tie points. Tie points will be selected in a set of correlation points, therefore, for all images, a correlation grid Γ_c is computed using all the nodes of the grid Γ .



Figure 9 – Recovering zone: Iteration 4



Figure 10 – Results of the algorithm, useful zone to look for tie points

The coordinates in the geometry of the secondary image can be found using the correlation grid information and the re-sampling grid information in three steps:

1. reading the positioning in the grid Γ_s
2. calculating the partial derivatives in order to change the geometry (from reference to secondary)
3. conversion (and addition) of the differences computed in the grid Γ_c applying the partial derivatives.

A set of correlations points is now available (Figure 11). These points can be described in any geometry. To do things properly, the correlation points are filtered. The nadir zone Λ is divided in a regular mesh (250x250 pixels i.e. $7 \times 17 = 119$ partitions). In each partition, the best tie point meets the following criteria:

- maximization of the number of ties with all the other images (4.83 ties on average)
- maximization of the product of the correlation coefficients (this criterion penalizes non homogeneous correlation points).

A set of tie points is available in each image of the block (Figure 12).

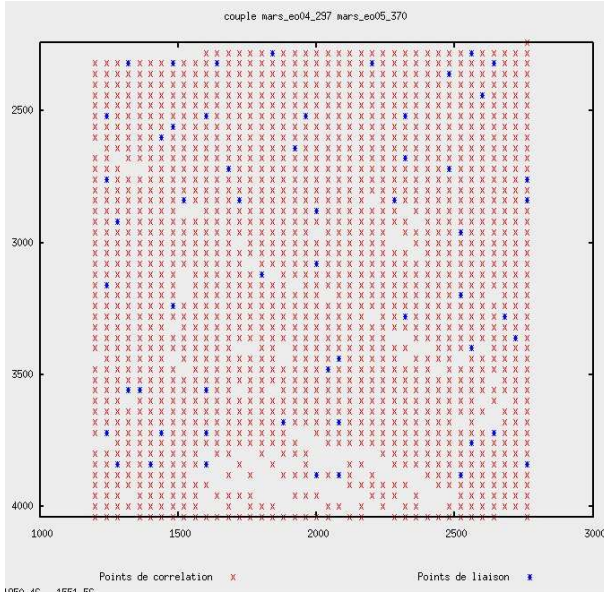


Figure 11 – Example of correlation point filtering: tie points (dark *) and correlation points (grey x) in the nadir zone of a reference image

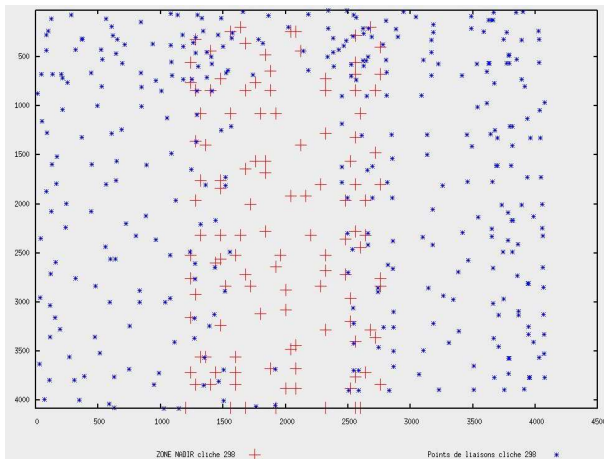


Figure 12 – Example of tie points computed for an entire image, the (+) are the tie points selected in the nadir zone

3.4 Aerotriangulation

Parameters

The block of the aerotriangulation holds 762 images, 87392 points and 422515 ties.

The standard deviation (σ_{te}) used for the tie equations in the aerotriangulation lies between 0.7m and 2.2m. This value depends on the correlation coefficient. If the correlation coefficient (cc) is more than 0.95 then the σ_{te} becomes 0.7m, otherwise the standard deviation is defined in an empiric way by $\sigma_{te} = \sqrt{100(1 - cc)}$.

The standard deviation used for the ground control point equations in the aerotriangulation are (0.1m ; 0.1m).

The constraints on the ground control points are (0.1m ; 0.1m) and 0.4m in altitude.

The constraints on the tie point altitudes are 20m.

The constraints on the trajectory are 100m in each direction.

Finally, the constraints on the models are 1m in each direction for the principal points and 0.1rd for the orientation of the camera (R, P, Y).

Some results

373027 ties were kept after a 3σ filtering of the aerotriangulation.

The RMS on ties are:

Along X (longitude) = 0.060m

Along Y (latitude) = 0.048m

The RMS on the ground control point equations are:

Along X (longitude) = 0.047m

Along Y (latitude) = 0.031m

The RMS on the ground control points are:

Longitude = 0.057m

Latitude = 0.054m

Altitude = 0.272m

4. 3D REFERENCE

4.1 Objectives

The main goal of this part is to build the best 3D geometric reference as possible to calibrate spatial sensor. At the end of the aerotriangulation, all the geometric models are accurate and we have correlation measurements at 10m.

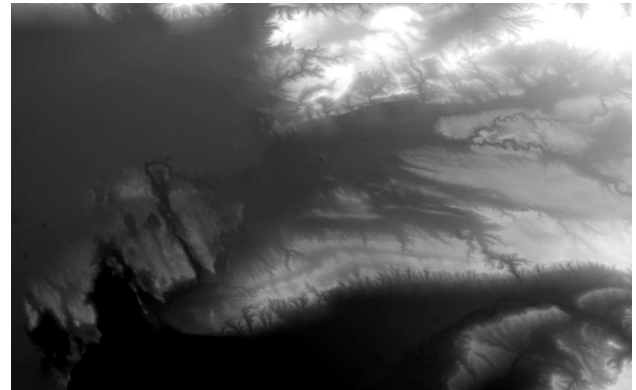


Figure 13 – BDTopo[®] DEM of the region of Salon de Provence

4.2 Methodology

The desired accuracy DSM production is composed of three main steps.

1. First a DSM at 10m is created from all the correlations used previously. For all images, and for all nodes of Γ , a 3D intersection of the viewing directions is calculated on the initial DEM. This method is detailed in the next paragraph. Some accuracy criteria are associated to each intersection like the number of viewing direction involved in the calculation, the average of the correlation coefficients associated to each node, the maximum of parallax used... The irregular grids computed are regularized, and then all the regularized grids are concatenated. The algorithm used is detailed in the next paragraphs.
2. Then a DSM at 1m is created using a thin correlation (4x4 pixels) between one image (the reference image and geometry) and the next image on the same band (the secondary image and geometry). The secondary

image is then projected in the geometry of the reference image using the DSM at 10m. After that a DSM at 1m is calculated using the method described in step 1.

3. At the end, the DSM at 1m is filtered, smoothed and filled up. To do that, absurd isolated altitudes are removed. Each connected zone is filled up by the best plan (least square meaning). This method is efficient on the water and homogeneous surfaces.

4.3 Viewing directions intersection

The intersection of the viewing directions described in step 1 and 2 of the DSM construction is resolved like the following problem.

Let Δ be a line passing through a point S and whose direction vector is \vec{V} , any point M and δ the distance between M and Δ .

Then,

$$\begin{aligned}\delta^2 &= \|\overline{SM} \wedge \vec{V}\|^2 = \overline{SM}^2 - (\overline{SM} \cdot \vec{V})^2 \\ d(\delta^2) &= 2(\overline{SM} \cdot d\vec{M} - \overline{SM} \cdot \vec{V} \cdot d\vec{M} \cdot \vec{V}) = 2d\vec{M} \cdot (\overline{SM} - \overline{SM} \cdot \vec{V} \vec{V}) \\ d(\delta^2) &= 2d\vec{M} \cdot (\overline{SM} - VV^t \overline{SM}) = 2d\vec{M} \cdot [(Id - VV^t) \overline{SM}] \\ d(\delta^2) &= 2d\vec{M} \cdot [(Id - VV^t) (M - S)]\end{aligned}$$

For a set of n of viewing directions Δ_i with (S_i, \vec{V}_i) , we are looking for as intersection of these viewing directions the point M which minimizes this distance quadratic sum:

$$\sum_i \delta_i^2 = \sum_i \|\overline{S_i M} \wedge \vec{V}_i\|^2 = \sum_i [\overline{S_i M}^2 - (\overline{S_i M} \cdot \vec{V}_i)^2]$$

Moreover,

$$\begin{aligned}d\left(\sum_i \delta_i^2\right) &= 2d\vec{M} \cdot \left[\sum_i (Id - V_i V_i^t) (M - S_i)\right] \\ d\left(\sum_i \delta_i^2\right) &= 2d\vec{M} \cdot \left[\sum_i (Id - V_i V_i^t) M - \sum_i (Id - V_i V_i^t) S_i\right]\end{aligned}$$

The solution is obvious:

$$M = \left[\sum_i (Id - V_i V_i^t)\right]^{-1} \sum_i [(Id - V_i V_i^t) S_i]$$

The real interest of this method is the simplicity of the algorithm:

- it is easy to compute the terms $Id - V_i V_i^t$ and $(Id - V_i V_i^t) S_i$
- only one 3x3 matrix inversion arises
- in an iterative process it is really easy to eliminate “far viewing directions” by removing the contribution of these viewing directions using the terms $\sum_i (Id - V_i V_i^t)$ and $\sum_i [(Id - V_i V_i^t) S_i]$.

4.4 Regularization method

The regularization of the DSM described in step 1 and 2 is presented in Figure 14.

A regular grid Γ_m is defined. Each node of the irregular grid is assigned to the four neighbour nodes of Γ_m (in a 4-connex neighbourhood) with an empirical coefficient K . This coefficient relies on distance between the nodes and criteria described in the step 1.

Nodes of Γ_m are computed using the weighted average by the K coefficients of the 0 to 4 neighbours. A quality index is also associated to each node of Γ_m .

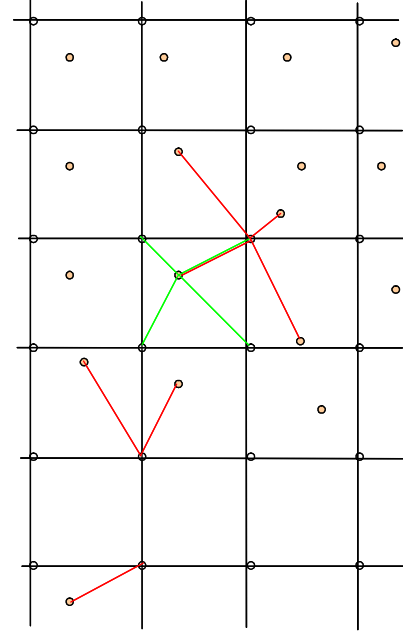


Figure 14 – Regularization of the meshed DSM

4.5 Some results

The algorithm previously described is applied on the block of Salon de Provence with 762 images. The DSM obtained is presented Figure 15. This can be compared to the initial DEM showed Figure 13. Extracts (Figure 16 and Figure 17) shows all the details of the DSM. The DSM obtained, at one meter ground resolution, has an altimetric accuracy better than 10cm RMS.

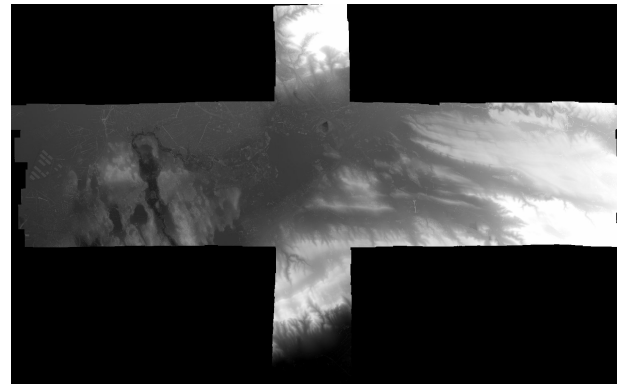


Figure 15 –Supersite of Salon de Provence DSM

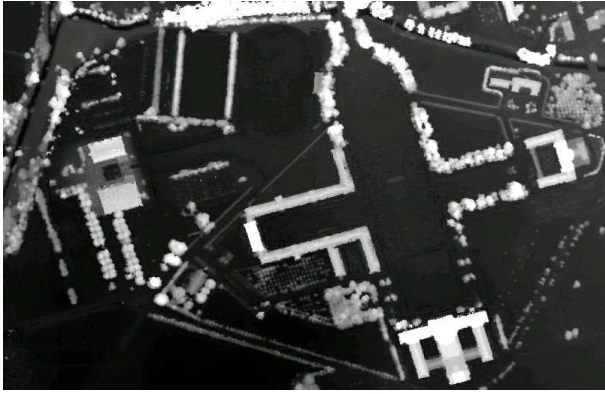


Figure 16 – Supersite DSM extract: the school of Salon de Provence



Figure 17 – Supersite DSM extract: Miramas

5. CONCLUSION

The aerotriangulation and the DSM allow us to have a high resolution geometric reference in order to calibrate any high resolution spatial sensor. We have all the elements to build an ortho-mosaic image, for example. The supersite of Salon de Provence suits geometric and radiometric image quality assessment and ensures an acceptable weather. It also ensures both planimetric and altimetric accuracy which are key factors for the geometric quality of a spatial sensor calibration. This supersite will be used to calibrate a spatial sensor like Pleiades.

6. REFERENCES

Gachet R., 1999, Caractérisation des Directions de Visée, Seminar «In-Orbit Geometric Characterization of Optical Imaging Systems» Bordeaux, 2-5 Nov 1999, SFPT bulletin n°159

Gachet R., 2004, SPOT5 in-flight commissioning : inner orientation of HRG and HRS instruments, ISPRS Congress Istanbul 2004